Environ Earth Sci (2014) 71:1925–1936
DOI 10.1007/s12665-013-2596-4

ORIGINAL ARTICLE

Hydrodynamic behavior of Kangan gas-capped deep confined aquifer in Iran

Arash Nadri · Rahim Bagheri · Ezzat Raeisi · Seyyed Shahaboddin Ayatollahi · Kamal Bolandparvaz-Jahromi

Received: 13 January 2013 / Accepted: 1 June 2013 / Published online: 15 June 2013

Abstract The Kangan aquifer (KA) is located beneath the Kangan gas reservoir (KGR), 2,885 m below the ground surface. The gas reservoir formations are classified into nine non-gas reservoir units and eight gas reservoir units based on the porosity, water and gas saturation, lithology, and gas production potential using the logs of 36 production wells. The gas reservoir units are composed of limestone and dolomite, whereas the non-gas reservoir units consist of compacted limestone and dolomite, gypsum and shale. The lithology of KA is the same as KGR with a total dissolved solid of 333,000 mg/l. The source of aquifer water is evaporated seawater. The static pressure on the Gas–Water Contact (GWC) was 244 atm before gas production, but it has continuously decreased during 15 years of gas production, resulting in a 50 m uprising of the GWC and the expansion of KA water and intergranular water inside the gas reservoir. The general flow direction of the KA is toward the northern coast of the Persian Gulf due to the migration of water to the overlying formations via a trust fault. The KA is a gas-capped deep confined aquifer (GCDCA) with special characteristics differing from a shallow confined aquifer. The main characteristics of a GCDCA are unsaturated intergranular water below the confining layers, no direct contact of the water table (GWC) with the confining layers, no vertical flow via the cap rock, permanent uprising of the GWC during gas production, and permanent descend of GWC during water exploitation.

Keywords Gas-capped deep aquifer · Kangan gas reservoir · Hydrodynamics · Formation water · Gas water contact · Flow direction

A. Nadri · R. Bagheri · E. Raeisi (✉)
Department of Earth Sciences, College of Sciences, Shiraz University, Shiraz, Iran
e-mail: e_raeisi@yahoo.com

S. S. Ayatollahi
Petroleum and Chemical Engineering, College of Engineering, Shiraz University, Shiraz, Iran

K. Bolandparvaz-Jahromi
South Zagros Oil and Gas Company, Iranian Oil Company, Shiraz, Iran

Introduction

The Hydrodynamics of fluid flow in sedimentary basins is important because of its significant role in the formation and accumulation of hydrocarbons, waste water, and CO_2 storage in geologic formations and the management of gas and oil reservoirs (Villegas et al. 1994; Saripalli et al. 2001; Bachu et al. 2007; Khan and Rostron 2004; Yang et al. 2011; Hou et al. 2012; De Lucia et al. 2012; Novak et al. 2013). The hydrodynamic information of aquifers in hydrocarbon reservoirs seems to be limited to hydraulic head, water driving forces, general groundwater direction, salinity maps, and sources of water salinity (Bachu and Underschultz 1993; Bachu 1997; Anfort et al. 2001; Berg et al. 1994; Villegas et al. 1994; Bachu and Hitchon 1996; Birkle et al. 2002, 2009; Carpenter 1978; Clayton et al. 1966; Fontes and Matray 1993; Kharaka and Hanor 2004; Knauth and Beeunas 1986). Formation water flows in sedimentary basins due to hydrodynamic and chemical potentials (Bjørlykke 1993). The hydrodynamic potential is caused by meteoric water flow (topographic differences), compaction-driven flow, and density-driven (buoyancy) flow (Bjørlykke 1993; Bachu 1995a, b). Villegas et al. (1994) applied the principles of stratigraphy, lithology, fluid and rock

properties, geothermal data, and hydraulics to study the regional-scale hydrodynamics of the Llanos basin in Colombia, Canada. They showed that the topography differences and the buoyancy resulting from temperature differences are the driving forces behind the formation-water flow in the Llanos basin. They also concluded that the basin-scale flow of formation waters has contributed to the present day distribution of hydrocarbons in the basin.

Bachu and Hitchon (1996) studied basin-scale flow of formation waters in the Williston basin in the United States–Canada border in the northern Great Plains—Prairie region of North America, using salinity and pressure data. They concluded that the main driving force behind formation-water flow in the basin is the basin topography, driving the water from the recharge areas to the discharge areas. Bachu and Underschultz (1993) used formation-water analysis, drill stem tests, and core plug data to study the hydrogeology of formation waters of the northeastern Alberta basin. They concluded that topography and buoyancy effects are the main driving forces for deep formation-water flow in northeast of the Alberta basin. Buoyancy force opposes the topographically-induced formation-water flow. They also concluded that the formation-water flow in the northeastern edge of the basin plays an important role in the migration of hydrocarbons and the formation of Athabasca oil sand deposits.

The change in depth of gas (oil)–water contact (GWC) can be the result of reservoir compartmentalization, faulting, or stratigraphic barriers, or it may be the result of a hydrodynamic aquifer and formation-water flow (Knipe et al. 1998; Jolley et al. 2007; Muggeride and Mahmode 2012). Hubert (1953) described the effect of a hydrodynamic aquifer on the tilt of an oil–water contact (OWC). This effect has been observed in many basins around the world (Dahlberg 1995; Chiarelli 1978; Seggie et al. 2000). Berg et al. (1994) studied the hydrodynamic behavior of regional formation flow and its effects on the tilted OWC in the Billing Nose area in Dakota. They found that the gradient of the GWC tilt is about 5 m/km, approximately equal to the regional topography gradient. They concluded that the formation-water flow of the hydrodynamic aquifer below the OWC caused a tilted OWC in the region. Tozer and Borthwick (2010) studied the fluid contacts in the Azeri gas field of Azerbaijan. They found that there is 3.5 bar/km water potential gradient in the field that is a result of formation-water flow.

There are limited studies regarding the hydrodynamics of reservoirs in the Persian Gulf region. Pelissier et al. (1980) studied the hydrodynamics of the Mid-Cretaceous oil reservoirs (Fateh, Sirri-C and Sirri-D) in the Persian Gulf region. They showed that there is a strong hydrodynamic flow of formation water toward the central regions of the Persian Gulf. Similarly Wells (1988) studied the Mid-Cretaceous offshore oil reservoirs of Qatar and showed that the hydrodynamics of formation waters indicate a flow toward the central regions of the Persian Gulf.

The Kangan gas field, composed of Permian to Triassic Formations, is located in the south of Iran. It is the largest onshore gas condensate reservoir in the Middle East. The Kangan aquifer (KA) and Kangan gas reservoir (KGR) are interrelated and complicated hydraulic systems. In this comprehensive work, we study the hydrodynamics of the KA and gas reservoir using all of the available data including lithology, pressure, porosity, water and gas

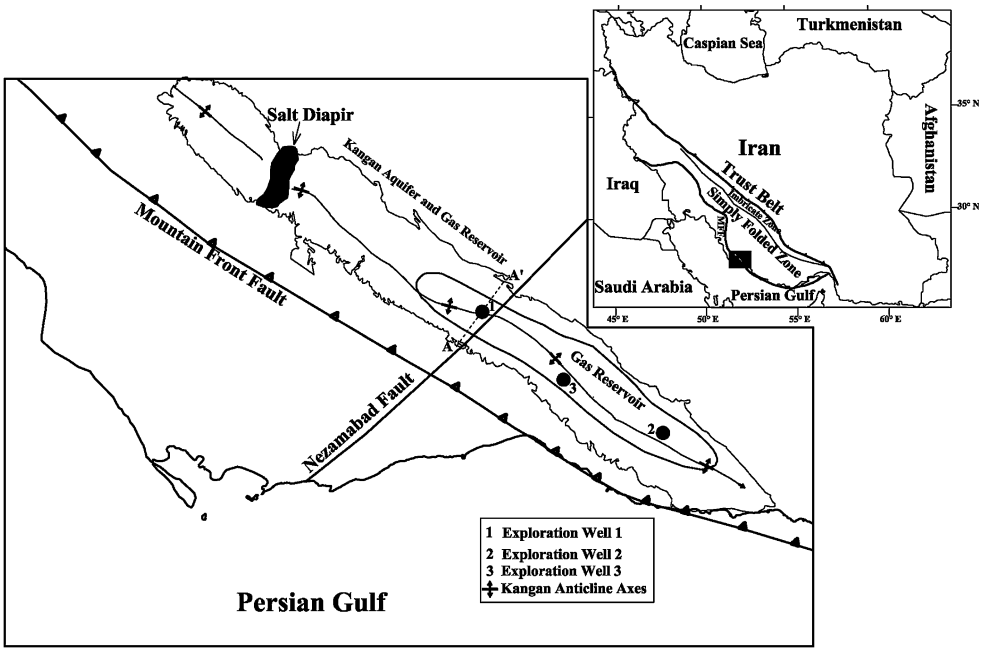

Fig. 1 General location map of the KA and KGR

saturation, GWC, and the initial static pressure of nearby hydrocarbon fields. In addition, the regional flow direction is discussed.

Geology of the Kangan aquifer and gas reservoir (KAGR)

The Zagros Highland occupies the borderlands of Iran, from eastern Turkey to the Oman Sea. The Zagros orogenic system may be divided longitudinally into the Simple Folded Zone, Imbricated Zone, and Thrust Zone. The Simple Folded Zone, the southwestern half of the orogenic system, is a zone of strong folding produced for the most part by Late Pliocene orogeny. This zone is characterized by a repetition of long and regular anticline and syncline folds (Raeisi 2008; Miliaresis 2001). The Kangan anticline is situated in the Zagros Simple Folded Zone (Figs. 1, 2), which is formed by compressional tectonics during the Miocene (Talbot and Jarvis 1984). The stratigraphic and structural settings of the Zagros sedimentary sequence have been described in detail by James and Wynd (1965), Falcon (1969, 1974), Stocklin and Setudehnia (1977), Motiei (1993) and Alavi (2004). The geological column of the Zagros Zone is presented in Fig. 3 (Bordenave 2008; Alavi 2004). The Milla, Ilbeyk, and Zardkuh Formations are reported in the general geological column of the Zagros range, but their existence in the study area is uncertain due to the lack of outcrops or constructed wells up to the possible location of these formations. The Kangan anticline, with an area of about 900 km^2 (90 by 10 km), follows the general NW–SE trend of the Zagros Range (Fig. 1). The outcropped formations are shown in Fig. 2.

The KA and gas field and their adjacent formations, in decreasing order of age, are the Hormuz, Sarchahan (Silurian Shale), Zakeen, Faraghan, Dalan, Kangan, and Dashtak Formations (Fig. 3). These formations are discussed here in detail due to their importance in the hydrogeology of the KA. The detailed information of these formations has been congregated by analyzing geological logs of 36 production wells, three exploration wells, and available literature (Stocklin and Setudehnia 1977; Stocklin 1968; Kent 1979; Motiei 1993). The Hormuz Formation, with a thickness of 900–1,500 m, is a complex of rock salt which was deposited on the rifted continental margins of the Arabian Plate in a rectangular basin during the Upper Precambrian to Middle Cambrian (Stocklin 1968). Salt has a low density of 2,165 kg/m^3. Consequently, when it is subjected to considerable lithostatic pressure, the salt tends to flow upward along faults. The displaced salt may reach the ground surface in the form of diapirs (Kent 1958, 1979). A salt diapir, namely Kuh-e-Namak, extruded in the western region of the Kangan anticline far away from the

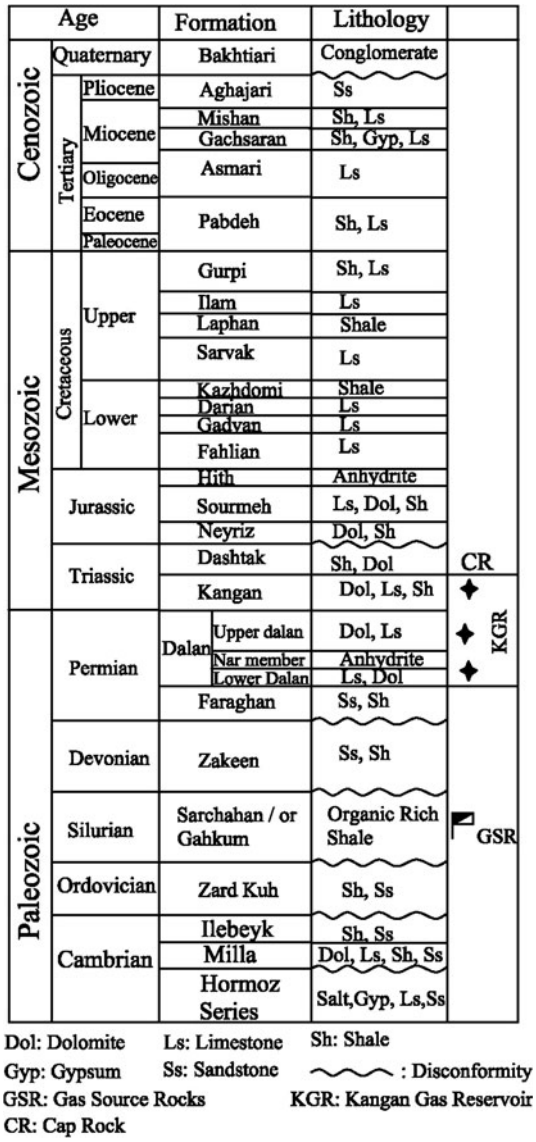

Fig. 2 Stratigraphic column of the study area

KGR (Figs. 1, 2). The Kuh-e-Namak salt diapir started to rise up through 8–10 km of folded Phanerozoic sediments since Jurassic (Talbot 1979). The Paleozoic deposits consist of the Silurian bituminous shale and the Lower Devonian to Lower Permian Faraghan Formations. The Silurian Shale (Sarchahan Formation) is the gas source rock (Boredenave and Hegre 2010), and it is the result of the deposition of low-energy graptolite sediments. These laminated graptolite shales are organic-rich and highly pyritic. After the deposition of the Early Miocene, huge quantities of gas were generated from the Silurian Shales (Boredenave and Hegre 2010). The lower half of the Devonian Zakeen Formation is dominantly sandy and is interpreted to have been deposited in a supratidal to subtidal environment. Mud-dominated deposits laid down in a slightly deeper environment are present in the upper part of

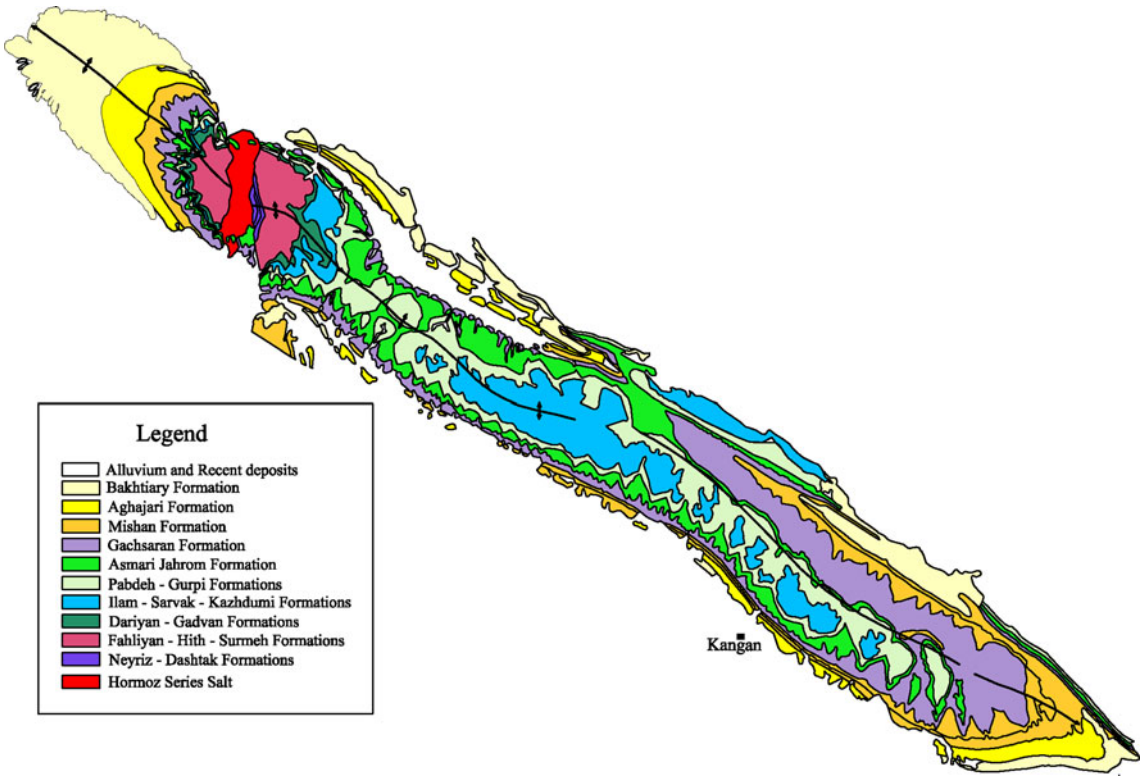

Fig. 3 Geological map of the study area

the Zakeen Formation (Bordenave 2008). The Early Permian Faraghan Formation, with a thickness of 113 m, consists of alternations of sandstone, shale, and limestone (Aali et al. 2006; Motiei 1993). The Faraghan Formation is overlain by the Dalan Formation and rests disconformably on the Mud-dominated deposits of the Zakeen Formation (Ghavidel-Syooki 2003). The Late Permian Dalan Formation, with a thickness of 755 m, is subdivided into three members: (1) Upper Dalan limestone, dolomite, and dolomitic limestones with thin layers of shale; (2) Nar anhydrite alternating with dolomite and limestone; and (3) Lower Dalan limestone (National Iranian Oil Company report 2007a). These three members have 250, 246, and 265 m thicknesses, respectively. The lower boundary of the Dalan Formation is transitional with the Faraghan, and the upper boundary is an erosional unconformity with the Kangan Formation (National Iranian Oil Company report 2007a). The Early Triassic Kangan Formation is mainly composed of limestone with alternative layers of dolomite, anhydrite, and shale. The thickness of the Kangan Formation is 215 m. The upper limit of the Kangan Formation is the Aghar Members of the Dashtak Formation. The Lower Triassic Dashtak Formation, with an average thickness of 725 m, has three main members: the Aghar Shale, the Blue Zone limestone and anhydrite, and the Sefidar dolomite. The shale of the Aghar Member, with a mean thickness of 25 m, is the efficient cap rock of the KGR (National Iranian Oil Company report 2007a).

There are two main faults, namely the Mountain Front Fault (MFF) and Nezamabad (Fig. 1). The MFF, a reverse basement trust fault, is located in the southern flank of the Kangan anticline parallel to the strike of the anticline (National Iranian Oil Company report 2009c). This fault is located at the foot of the anticline; therefore, it has no impact on the axes of the anticline, which is the host rock of the KGR. The Nezamabad Basement Fault (Fig. 1), with a deformed width of 8 km, intersects the anticline axes (Najafi 2009; National Iranian Oil Company report 2009c). Extensional faults have been formed along the anticline axes, with a few to 10 m displacements in which the fault plans have dips ranging from 50° to 80° (National Iranian Oil Company report 2009c). This group of faults has not extended into the surface layers and does not penetrate the KA. The correlations of lithological units in 36 production wells showed that the two mentioned faults have not caused any displacements in the KGR.

Method of study

The static pressures were measured using pressure gage in the gas wells, after the wells have been closed for a period

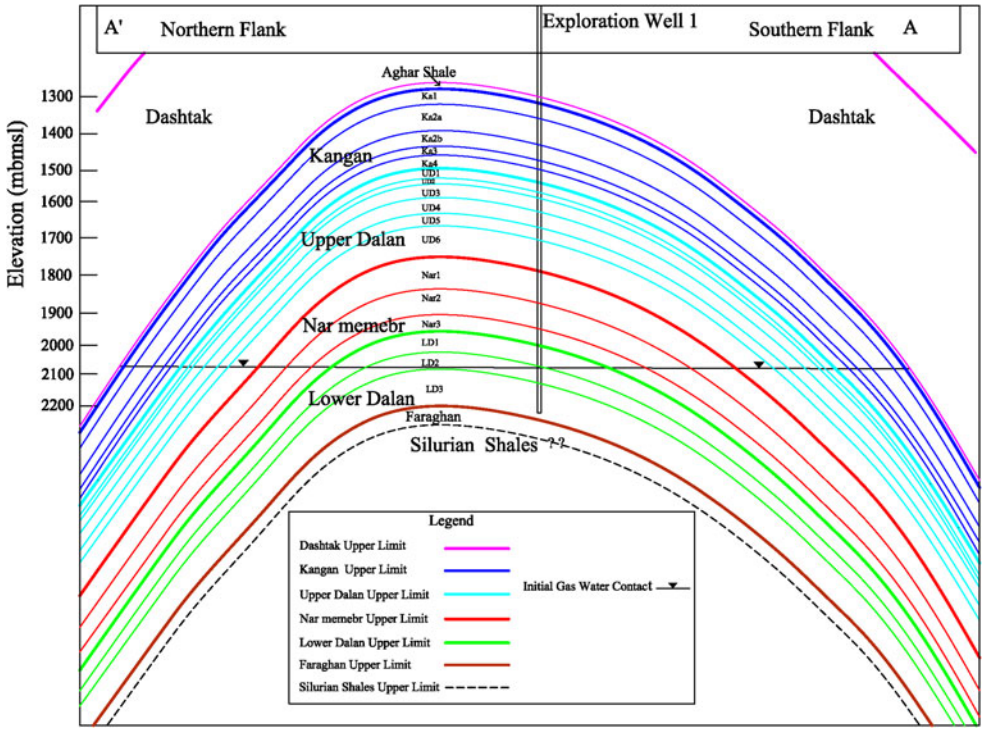

Fig. 4 Geological cross-section of the Kangan aquifer and gas reservoir, presenting the Kangan and Dalan units (*AA′* is presented in Fig. 1)

of 24–72 h. Drill stem tests (DST) were used to determine the gas potentials of newly drilled gas wells. Acquired from DST were samples of reservoir fluid, and records of flowing- and static bottom-hole pressures. During the tests, the DST tool was attached to the drill string and lowered to the zone of interest and allowed the formation fluid to flow in. Then, the pressures and flow rates were recorded (Earlougher 1977). Chaudhry (2004) has presented a detailed chapter on DST data interpretation. The initial GWC (IGWC) was calculated based on the measurements of gas pressures at different depths of the exploration wells. The pressure data were plotted versus depth. The depth at which the pressure gradient significantly reduced indicated the GWC.

Two water samples were taken from exploration well no. 3, as the representative of the aquifer water. Gas flowed for a few hours to flash the old water in the wellbore. The bottom-hole sampling device was used to transport the brine sample to the surface. The water samples were filtered using 0.45 micron filters and collected in 400 ml dark polyethylene containers. For trace elements, the samples were acidified with HCl to a pH <2. The pH and electrical conductivity were measured at the field. Total dissolved solid was measured by the water evaporation technique. The major ions were measured using conventional methods in the laboratory of the Geosciences Department of Shiraz University. The trace elements were analyzed in the ACTLABS, Canada using the ICP-MS and ICP-OES techniques.

Results and discussion

The area of the gas reservoir is 370 km^2 (Fig. 1). Gas is trapped in the crest of the Kangan anticline in the Dalan and Kangan Formations (Fig. 4). The gas reservoir is limited to the Aghar Shale at the top and to the GWC at the bottom. The thickness between initial and the present GWC and the cap rock (Aghar Shale) vary in the different parts of the KGR, having a maximum thickness of 750 m. The Aghar Member, the cap rock of the KGR, is composed of shale with the maximum, minimum, and average thicknesses of 30, 20, and 23 m, respectively (National Iranian Oil Company report 2009a, b). The average porosity of 0.0009 and water saturation of 100 % confirms the cap rock characteristic of the Aghar Member. The cap rock has a higher entry pressure than the entry pressure of the underlying Kangan Formation, preventing gas flow through the cap rock. If the pore space is initially fully occupied with brine, the capillary pressure must be exceeded a finite value called the entry pressure, before gas phase can intrude into the pore spaces (Corey 1977).

The exploration well no. 1, 2, and 3 were drilled in 1972, 1974, and 1975, respectively, and the gas production

Table 1 Porosity, water and gas saturation, lithology, average thickness, and gas production potential in the Kangan and Dalan units

Formation	Layer	Porosity (%)			Water saturation (%)			Gas saturation (%)			Litology	Average thickness (m)	Gas production potential
		Minimum	Average	Maximum	Minimum	Average	Maximum	Minimum	Average	Maximum			
Dashtak	Aghar	0	0.0035	0.0236	–	100	100	–	0	0	Shale	25	Cap rock
Kangan	Ka1	0.34	1.27	3.01	19.59	30.68	56.41	43.59	69.32	80.41	Dolomite and shale layers	42	Low
	Ka2a	2.69	4.56	6.8	11.3	20.24	32.82	67.18	79.76	88.7	Dolomitic limestone	69	Good
	Ka2b	1.58	3.05	5.7	14.74	23.44	42.44	57.56	76.56	85.26	Dolomite and limestone	40	Good
	Ka3	3.66	7.52	10.25	12.78	18.78	28.6	71.4	81.22	87.22	Oolitic limestone	29	Very good
	Ka4	0.03	0.59	1.83	10.54	34.43	69.26	30.74	65.57	89.46	Very compacted clayey limestone	35	Low
Upper Dalan	UD1	0.01	0.65	1.53	18.59	41.6	99.97	0.03	58.4	81.41	Very compacted clayey limestone	35	Low
	UD2	1.2	3.36	5.37	17.68	32.94	59.34	40.66	67.06	82.32	Dolomitic limestone	19	Good
	UD3	0.06	1.56	6.56	11.75	34.45	67.45	32.55	65.55	88.25	Very compacted clayey limestone	36	Low
	UD4	2.81	5.14	7.16	8.93	18.11	38.41	61.59	81.89	91.07	Dolomitic limestone and limestone	44	Very good
	UD5	1.61	4.09	7.85	17.62	28.03	43.84	56.16	71.97	82.38	Dolomitic limestone	38	Good
	UD6	0.17	1.38	4.51	10.08	39.28	70.32	29.68	60.72	89.92	Compacted clayey limestone	73	Low
Nar	Nar1	0.33	0.95	2.27	8.17	11.03	22.27	77.73	88.97	91.83	Anhydrite and dolomite	–	Low
	Nar2	–	0.95	–	–	11.03	–	–	88.97	–	Anhydrite and dolomite	–	Low
	Nar3	–	0.9	–	–	90.2	–	–	9.8	–	Anhydrite limestone and dolomite	–	Low
Lower Dalan	LD1[a]	0.5	3.6	5	1	–	–	–	–	–	Anhydrite and dolomite	63	–
	LD2[a]	1	7	10	1	–	–	–	–	–	Dolomitic limestone	51	–
	LD3[a]	1	7.6	13	1	–	–	–	–	–	Dolomitic limestone	–	–

–, not available

[a] These units are only intersected in exploration well

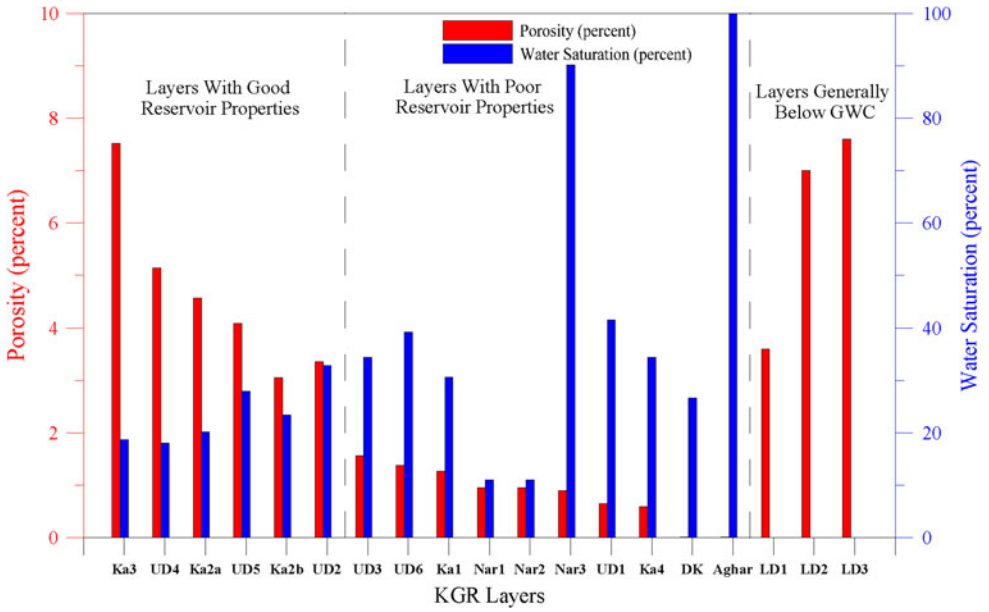

Fig. 5 Average porosity and water saturation of all of the gas production wells in the KGR

wells were drilled between 1987 and 2008. The porosity, water and gas saturation, lithology, average thickness, and gas production potential in the Kangan and Dalan Formations were measured in the gas reservoir and cap rock based on the logs of 36 production wells and three exploration wells data (National Iranian Oil Company report 2009a, b). The gas reservoir formations are classified into non-gas reservoir and gas reservoir units, based on the mentioned measured parameters (Table 1; Figs. 4, 5). The lithology of the gas reservoir units is limestone and dolomite, whereas the non-gas reservoir units consist of compacted clay limestone, anhydrite limestone and dolomite, dolomite and shale, and anhydrite and dolomite. The Kangan Formation is divided into the five units of Ka1, Ka2a, Ka2b, Ka3, and Ka4, with thicknesses from 29 to 69 m (Fig. 4; Table 1). Out of these five units, the Ka2a, Ka2b, and Ka3, with a lithology of limestone and dolomite, have the necessary characteristics of a gas reservoir. The Ka2 is divided into two sub units, namely Ka2a and Ka2b, due to the differences in their porosity and water saturation. The Dalan Formation consists of 12 units, the Upper Dalan (UD1–UD6 with thicknesses of 19–73 m), the Nar Members (Nar1–Nar3 with thicknesses of 55–106 m), and the Lower Dalan (LD1–LD3 with thicknesses of 51–145 m). The units with gas reservoir characteristics are the UD2, UD4, UD5, LD1, LD2, and LD3. The gas reservoir units are sandwiched between the non-gas reservoir units, but hydraulic connections exist between the gas reservoir units. This is because (a) parts of the non-gas reservoir units contain gas; (b) the non-gas reservoir units have small thicknesses; (c) equal static bottom-hole pressures prevail in the production wells at

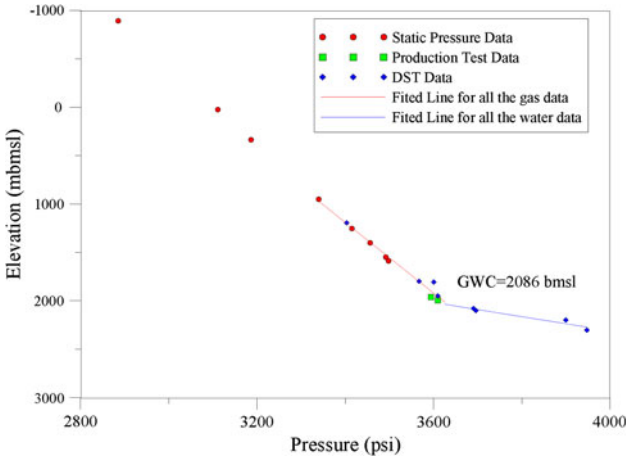

Fig. 6 Depth versus static pressure in exploration wells no. 1, 2, and 3

different depths; and (d) microfractures connect two alternative gas reservoir units. The average porosity of the non-gas reservoir and the gas reservoir units ranges from 0.59 to 1.56 % and from 3.05 to 7.52 %, respectively. Water saturation is higher in the non-gas reservoir units, except for units Nar1 and Nar2 having anhydrite and dolomite lithology (Figs. 4, 5; Table 1). The low water saturation of units with an anhydrite lithology is not expected and it merits more research.

The KA underlies the GWC in the gas reservoir area (Fig. 4) or the Aghar Shale of the Dashtak Formation out of the gas reservoir, and it most probably overlies the Silurian Shales. It is located 2,885 m below the ground. The aquifer formations are Dalan, Kangan, and Faraghan. No boreholes

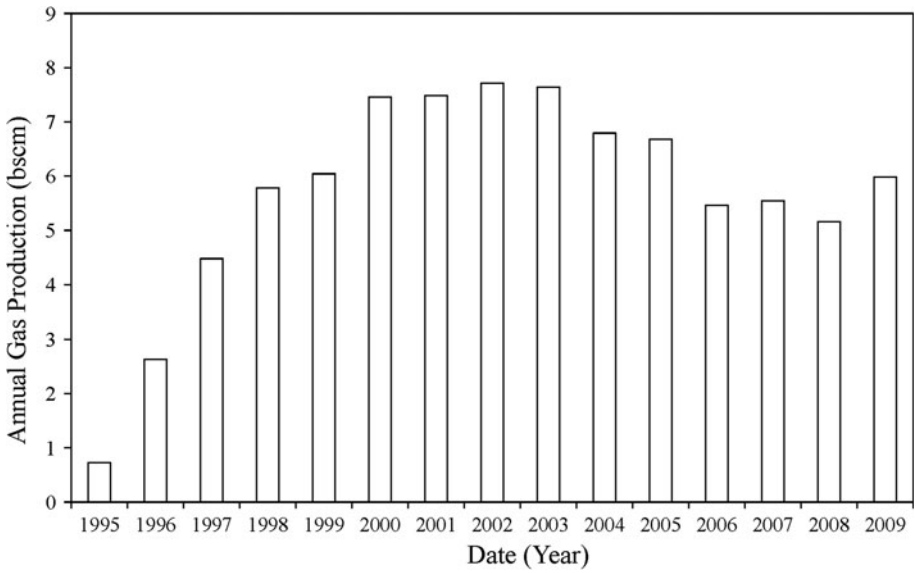

Fig. 7 Annual gas production of all of the gas production wells within the period of 1995–2009

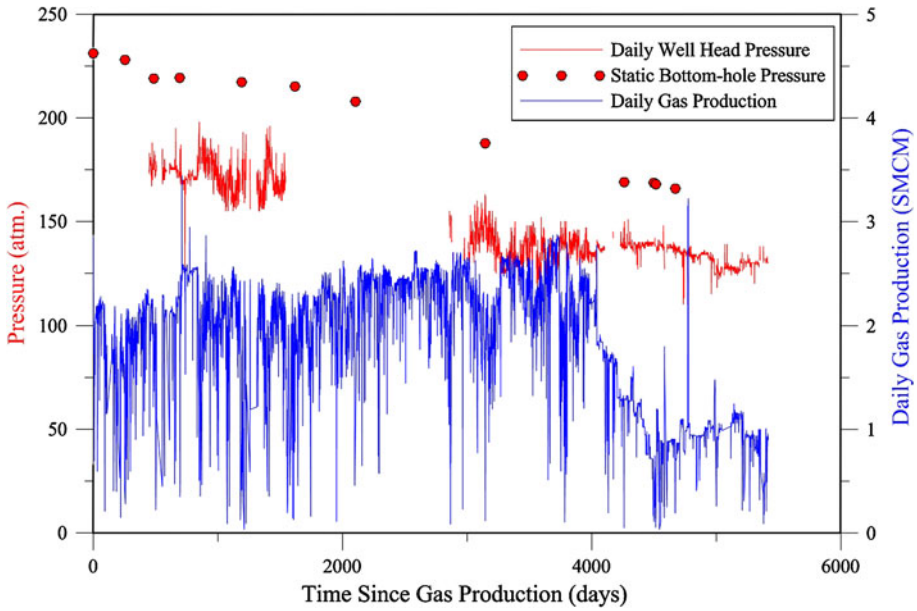

Fig. 8 Gas production, flowing well head pressure, and static bottom-hole pressure in exploration well no. 1

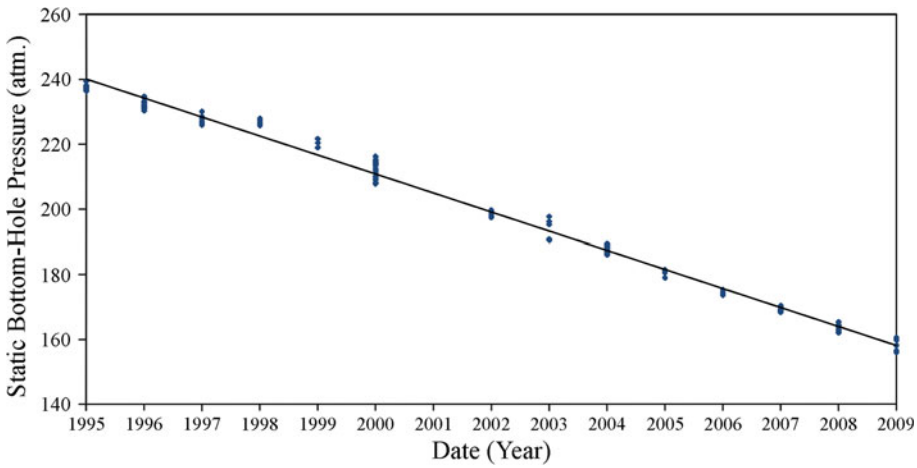

Fig. 9 The static bottom-hole pressure at the reference depth for all of the production wells from 1995 to 2009

Table 2 Concentration of the major ions, Br and I (mg/l), in exploration well no. 3

Sample date	HCO_3^-	Mg^{2+}	Ca^{2+}	SO_4^{2+}	Cl^-	Na^+	K^+	Br^-	I^-	TDS	Water type
11-23-2009	542	14,579	30,650	252	177,500	66,999	501	1,300	2.4	333,820	Na–Ca–Cl
4-29-2010	427	15,140	30,000	240	177,500	66,930	625	1,378	3.4	333,000	Na–Ca–Cl

were constructed inside the KA, but the geological units, lithology, and porosity are similar to the KGR. No precise data is available on the depths of the aquifer, but the thickness of the KA is at least 850 m, considering only the Kangan and Dalan Formations.

The depth of the IGWC was 2,075 m below mean sea level (mbmsl) in exploration well no. 1 using DST, static pressure, and production test data (National Iranian Oil Company report 2009b), and 2,084 mbmsl using the well logging method. The pressure data were not enough to calculate the IGWC in exploration wells no. 2 and 3. The accumulation of all of the data of these three exploration wells showed that the IGWC is 2,086 mbmsl (Fig. 6). The IGWC is selected to be 2,085 mbmsl based on the average of the well logging and pressure methods. The pressures and temperatures were measured at the GWC before gas production. The pressures in exploration wells no. 1, 2, and 3 were 243.8, 242.8, and 244.4 atm, respectively. The almost identical values of the pressures indicate hydraulic connectivity of all parts of the KGR and, practically, identical elevation of IGWC for all parts of the KGR. The temperature ranges from 82 to 87 °C in exploration wells no. 2 and 3 using DST.

Gas production was initiated in 1995. The annual gas production of the Kangan gas field is presented in Fig. 7. The total gas production was about 85.6 billion standard cubic meters (bscm) from 1995 to 2009. A typical daily time series of gas production, well head flow pressure (WHFP), and bottom-hole static pressure (BSP) is presented in Fig. 8 for production well no. 1. The WHFP continuously decreased in all of the wells with gas production, with the pressure gradient being dependant on the production rate. The BSP of all of the production wells at the reference depth of 1,800 mbmsl are presented in Fig. 9. The average pressure drop rate of BSP is 5.71 atm/year, and the total pressure drop is 80 atm during 14 years of gas production.

The GWC was only measured four times in exploration well no. 3 during a 12-year period. The GWC rose by 50 m from 1995 to 2006. Assuming a constant GWC uprising rate, the average GWC increment is about 4.16 m/year. The average GWC uprising was 0.71 m per 1 atm static pressure drop during the study period. The main reason of GWC uprising is gas production and consequently, pressure drops and expansion of water in the KA. In addition, the pressure drop expands the intergranular water inside the gas reservoir; therefore, the water saturation increases. The rising GWC may kill the gas productive wells in the future. For example, well no. 28 has the smallest initial distance between IGWC and the bottom of the well pay zone (113 m). Assuming the same trend for the GWC uprising rate, the GWC will reach the well pay zone and practically kill this well in 2022.

Table 3 Concentration of trace elements (mg/l) in decreasing order of concentration in exploration well no. 3

Sample date	Sr^{2+}	Zn^{2+}	Li^+	Rb^+	Mn^{3+}	Ba^{2+}	Pb^{2+}	Se^{2-}	Cu^+
23-11-2009	1,253	357	129	22.9	18.6	16.3	6.7	2.4	0.77
5-4-2010	1,450	165	152	20.5	19.1	14.2	1.2	0.5	0.10

Several water samples were taken 54 and 183 m below the GWC during drilling of exploration wells no. 2 and 3 using the DST method (National Iranian Oil Company report 2009b). The average total dissolved solid (TDS) values were 300,000 and 330,000 mg/l, respectively. In addition, two more water samples were taken from observation well no. 3 during this study. The major ions and tracer elements of these water samples are presented in Tables 2 and 3. The TDS was about 333,000 mg/l and the type of water was sodium–calcium chloride. The percentage of calcium, sodium, and chloride was 10.5, 23, and 60.9 %, respectively. The average concentration of bromide was 1,320 mg/l. The source of brine water is evaporated seawater (Bagheri 2013). The most common trace elements, in decreasing order of concentration, are Sr^{2+}, Zn^{2+}, Li^+, Rb^+, Mn^{3+}, Ba^{2+}, Pb^{2+}, Se^{2-}, and Cu^+.

The Permo–Triasic Formations are extensive gas reservoirs in the Persian Gulf region. These include the Dalan and Kangan Formations in southern Iran, and their equivalent, the Khuff Formation in the southern coast of the Persian Gulf (Insalaco et al. 2006; Sharland et al. 2001; Ehrenberg et al. 2007; Boredenave and Hegre 2010; Alavi 2007; Rahimpour-Bonab et al. 2010). A restricted lagoon was developed during the Permian, extending along the whole Arabian platform. The Lagoon turned into a sabkha environment due to warm and dry climatic conditions (Szabo and Kheradpir 1978; Boredenave and Hegre 2010). Therefore, a great brine aquifer developed in the Kangan and Dalan (Khuff) Formations. The Early Silurian Shale (Sarchahan Formation), which is mainly composed of

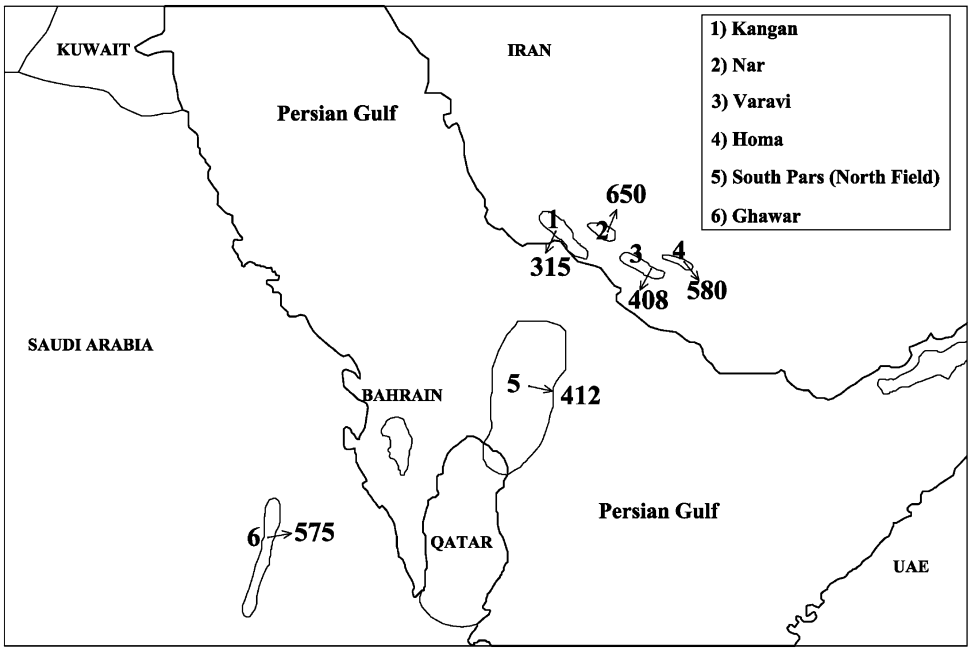

Fig. 10 Location map of several gas reservoirs in the vicinity of the KA, with data of the total pressure head at the GWC

organic-rich black shales, is identified as the source rock for most of the huge gas reserves in the Paleozoic strata of southern Iran (Mahmoud et al. 1992). The produced gas in the Sarchahan Formation migrated to the Dalan and Kangan carbonate formations and formed huge gas caps in the crest of the anticlines above the pre-existing brine aquifer. The main Permo–Triasic gas reservoirs are Kangan, Nar, Varavi, Shanul, Mond, North Pars, Assaluyeh, Homa, Tabnak, and Lavan, Kish in southern Iran, South Pars (North Dome) shared by Iran and Qatar, and Ghawar in Saudi Arabia. The data of the GWC elevation (Z) and gas pressure on the surface of the GWC (P) before gas production are available for the gas hydrocarbon fields of Nar, Homa, Varavi, (National Iranian Oil Company report 2007a, b, c, 2009b), and South Pars (North Field) and Ghawar (Whitson and Kuntadi 2005). The total head (H) was calculated using the following equation (Bachu and Michael 2002):

$$H = z + P/(\rho \times g)$$

in which ρ is the fresh water density. The total heads of the Kangan and adjacent gas fields are presented in Fig. 10. The total heads at the GWC of Nar and Homa, and the Ghawar and North Field (South Pars) gas fields are 650, 580, 475 and 412 m, respectively, whereas the Kangan and Varavi gas fields have the lowest total heads of 315 and 408 m, respectively. This implies that the general flow of aquifer brines is in the opposite direction toward the north coast of the Persian Gulf (Fig. 10). The flow of water only occurs where the aquifer water rises up toward the overlying formations of Kangan and Dalan. The reverse basement trust MFF is located at the southern flank of the Kangan anticline. There are no gas reservoirs along this fault; therefore, the brine aquifer is transferred to the overlying formations, especially in the Dashtak Formation via this fault.

Conclusions

The Kangan brine aquifer underlies the KGR which is trapped at the crest of the Kangan anticline. The KA is composed of Kangan, Dalan, and the underlying sandstone Faraghan Formations, with the water type being sodium–calcium chloride and having a TDS of 333,000 mg/l. The IGWC was located at an elevation of 2,085 mbmsl. The KGR consists of the Kangan and Dalan Formations. This reservoir is classified into nine gas reservoir units composed of limestone and dolomite, and eight non-gas reservoir units with a lithology of compacted limestone and dolomite, gypsum, and shale. The gas reservoir units have lower water saturation and higher porosity than the non-gas reservoir units. The cap rock is Aghar Shale, having very low porosity and being saturated with water. The static pressure of KGR was 240 atm before gas production.

The KA is a gas-capped deep confined aquifer (GCDCA) located 2,885 m below the crest of the Kangan anticline. The KA is a part of a great regional brine aquifer developed in the Kangan and Dalan Formations (equivalent to the Khuff Formation) in southern Iran, offshore and inshore of the Persian Gulf. This great regional aquifer is located beneath the gas reservoirs in the crest of some of the anticlines. The total pressure head on the GWC indicates that the general flow direction in the Kangan and Dalan (Khuff) Formations is toward the northern coast of

the Persian Gulf. The aquifer brine most probably migrates to the overlying formations via the MFF. The GCDCA has the following special characteristics compared to a shallow confined aquifer (SCA):

1. The upper boundary of the GCDCA is a high pressure gas cap where the upper boundary of SCA is a saturated impermeable or a semi-confining layer.
2. Water with high pressure is in direct contact with the confining layers in SCA and based on the Darcy equation; the water has the potential to flow through the confining layers. However, in the GCDCA, the water is undersaturated below the confining layers and the water entry pressure (P_e) in the gas reservoir is lower than the water entry pressure of the 100 % saturated confining layers, preventing the flow of gas and water through the confining layers.
3. The SCA is recharged by recycled meteoric water. Therefore, its piezometeric surface has a limited fluctuation range, except under overexploitation conditions. However, the gas or water exploitation in the GCDCA results in a permanent declining trend in static pressure. The initial BSP in the Kangan reservoir was about 244 atm on the GWC, decreasing to 164 atm during the 14 years of gas production of 85.6 bscm. The average BSP drop is 5.71 atm/year.
4. The significant gas pressure drop during gas production resulted in a decreasing water density, and consequently, the water expansion in the KA and KGR. Therefore, the GWC rose up, increasing the KA thickness. The uprising of the GWC depends on the thickness of the aquifer and the amount of gas pressure drop. In addition, the intergranular water occupies the larger pores in the gas reservoir units and water is released from the saturated non-gas reservoir units due to water expansion.
5. If the aquifer water is exploited from the GCDCA for a long period of time, the elevation of GWC permanently decreases below the gas reservoir region, resulting in the expansion of gas and intergranular water inside the gas reservoir.
6. The exploitation of gas or aquifer water decreases the pressure on the GWC, lowering the piezometeric surface in the GCDCA. Therefore, a local flow may occur toward the exploiting region.

Acknowledgments The authors extend their appreciation to the South Zagros Oil and Gas Company of Iran for the financial support of this study. The authors also thank A. Montaseri, M. Mirbagheri, H.R. Nasriani, Sh. Karimi and A.A. Nikandish, all from the South Zagros Oil and Gas Company, and Dr. A. Shariati and M. Escrochi from Shiraz University for their assistance in data acquisition, field work and extensive discussions on the characteristics of the Kangan Gas Reservoir. The authors also thank the Research Council of Shiraz University for continuous support during this investigation.

References

Aali J, Rahimpour-Bonab H, Kamali MR (2006) Geochemistry and origin of the world's largest gas field from Persian Gulf, Iran. J Petrol Sci Eng 50:161–175

Alavi M (2004) Regional Stratigraphy of the Zagros fold-thrust belt of Iran and its proforeland evolution. Am J Sci 304:1–20

Alavi M (2007) Structures of the Zagros fold-thrust belt in Iran. Am J Sci 307:1064–1095

Anfort SJ, Bachu S, Bentley LR (2001) Regional-scale hydrogeology of the upper Devonian–lower Cretaceous sedimentary succession, south-central Alberta basin, Canada. AAPG Bull 85:637–660

Bachu S (1995a) Synthesis and model of formation water flow in the Alberta basin, Canada. AAPG Bull 79:1159–1178

Bachu S (1995b) Flow of variable-density formation water in deep sloping aquifers: review of methods of representation with case studies. J Hydrol 164:19–39

Bachu S (1997) Flow of formation waters, aquifer characteristics, and their relation to hydrocarbon accumulations, northeastern Alberta basin. AAPG Bull 81:712–733

Bachu S, Hitchon B (1996) Regional scale flow of formation waters in the Wilinston basin. AAPG Bull 80:248–264

Bachu S, Michael K (2002) Flow of variable-density formation water in deep sloping aquifers: minimizing the error in representation and analysis when using hydraulic-head distributions. J Hydrol 259:49–65

Bachu S, Underschultz JR (1993) Hydrogeology of formation waters, northeastern Alberta basin. AAPG Bull 77:1745–1768

Bachu S, Bonijoly D, Bradshaw J, Burruss R, Holloway S, Christensen NP, Odd MM (2007) CO_2 storage capacity estimation: methodology and gaps. Int J Greenh Gas Control 1:430–443

Bagheri R (2013) Hydrochemistry and sources of connate water in the Zagros aquifers (PhD dissertation). Shiraz University, Shiraz

Berg RR, Demis WD, Mitsdraffer AR (1994) Hydrodynamic effects on Mission Canyon (Mississippian) oil accumulations, Billing Nose area, North Dakota. AAPG Bull 78:501–518

Birkle P, Aragon JJR, Portugal E, Aguilar JLF (2002) Evolution and origin of deep reservoir water at the Active Luna oilfield, Gulf of Mexico, Mexico. AAPG Bull 86:457–484

Birkle P, García BM, Padrón CMM (2009) Origin and evolution of formation water at the Jujo-Tecominoacán oil reservoir, Gulf of Mexico. Part 1: chemical evolution and water–rock interaction. Appl Geochem 24:543–554

Bjørlykke K (1993) Fluid flow in sedimentary basins. Sediment Geol 86:137–158

Bordenave ML (2008) The origin of Permo–Triassic gas accumulations in the Iranian Zagros fold belt and contiguous offshore areas: a review of the Paleozoic petroleum system. J Petrol Geol 1:3–42

Boredenave ML, Hegre JA (2010) Current distribution of oil and gas fields in the Zagros fold belt of Iran and contiguous offshore as the result of the petroleum systems. Geol Soc Lond Special Publ 330:291–353

Carpenter AB (1978) Origin and chemical evolution of brines in sedimentary basins. Okla Geol Surv Circ 79:60–77

Chaudhry AU (2004) Oil well testing handbook. Elsevier Inc, London

Chiarelli A (1978) Hydrodynamic framework of eastern Algerian Sahara influence on hydrocarbon occurrence. AAPG Bull 62:667–685

Clayton RN, Friedmann I, Graf DL, Mayeda TK, Meents WF, Shimp NF (1966) The origin of saline formation waters. J Geophys Res 71:3869–3882

Corey AT (1977) Mechanics of heterogeneous fluids in porous media. Water Resources Publications, Fort Collins

Dahlberg EC (1995) Applied hydrodynamics in petroleum exploration, 2nd edn. Springer-Verlag, Berlin

De Lucia M, Bauer C, Beyer C, Kühn M, Nowak T, Pudlo D, Reitenbach V, Stadler S (2012) Modelling CO_2-induced fluid–rock interactions in the Altensalzwedel gas reservoir. Part I: from experimental data to a reference geochemical model. Environ Earth Sci 67:563–572

Earlougher RC (1977) Advances in well test analysis (second printing). Society of Petroleum Engineers of AIME, USA

Ehrenberg SN, Nadeau PH, Aqrawi AAM (2007) A comparison of Khuff and Arab reservoir potential throughout the Middle East. AAPG Bull 91:275–286

Falcon NL (1969) Problems of the relationship between surface structure and deep displacements illustrated by the Zagros range. Geol Soc Lond Special Publ 3:9–21

Falcon NL (1974) Southern Iran, Zagros Mountains. In: Spencer AM (ed) Mesozoic–Cenozoic orogenic belts, vol 4. Geological Society of London Special Publication, London, pp 199–211

Fontes JC, Matray JM (1993) Geochemistry and origin of formation brines from the Paris Basin, France, 1. Brines associated with Triassic salts. Chem Geol 109:149–175

Ghavidel-Syooki M (2003) Palynostratigraphy of Devonian sediments in the Zagros Basin, southern Iran. Rev Palaeobot Palynol 127:241–268

Hou Z, Wundram L, Meyer R, Schmidt M, Schmitz S, Were P (2012) Development of a long-term wellbore sealing concept based on numerical simulations and in situ-testing in the Altmark natural gas field. Environ Earth Sci 67:395–409

Hubert MK (1953) Entrapment of petroleum under hydrodynamic conditions. AAPG Bull 37:1954–2026

Insalaco E, Virgone A, Courme B, Gaillot J, Kamali M, Moallemi A, Lotfpour M, Monibi S (2006) Upper Dalan Member and Kangan Formation between the Zagros Mountains and offshore Fars, Iran: depositional system, biostratigraphy and stratigraphic architecture. GeoArabia 11:75–176

James GA, Wynd JG (1965) Stratigraphic nomenclature of Iranian oil consortium agreements area. AAPG Bull 46:2182–2245

Jolley SJ, Barr D, Walsh JJ, Knipe RJ (2007) Structurally complex reservoirs: an introduction. Geol Soc Lond Special Publ 292:1–24

Kent PE (1958) Recent studies of south Persian salt plugs. AAPG Bull 422:2951–2972

Kent PE (1979) The emergent Hormuz salt plugs of southern Iran. J Petrol Geol 2:117–144

Khan DK, Rostron BJ (2004) Regional hydrogeological investigation around the IEA Weyburn CO_2 monitoring and storage project site. In: Rubin ES, Keith DW, Gilboy CF (eds) Proceedings of the 7th international conference on greenhouse gas control technologies (GHGT-7), vol 1, Vancouver

Kharaka YK, Hanor JS (2004) Deep fluids in the continents: I. Sedimentary basins. In: Drever JI (ed) Treatise in geochemistry, vol 5. Elsevier, London, pp 499–540

Knauth LP, Beeunas MA (1986) Isotope geochemistry of fluid inclusions in Permian halite with implications for the isotopic history of ocean water and the origin of saline formation waters. Geochim Cosmochim AC 50:419–433

Knipe RJ, Jones J, Fisher QJ (1998) Faulting, fault sealing and fluid flow in hydrocarbon reservoirs: an introduction. Geol Soc Lond Special Publ 147:7–21

Mahmoud MD, Vaslet D, Husseini MI (1992) The Lower Silurian Qalibah Formation of Saudi Arabia: an important hydrocarbon source rock. AAPG Bull 76:1491–1506

Miliaresis GC (2001) Geomorphometric mapping of Zagros ranges at regional scale. Comput Geosci 27:775–786

Motiei H (1993) Stratigraphy of Zagros. In: Hushmandzadeh A (ed) Treatise on the geology of Iran. Geological Survey of Iran, Iran

Muggeride A, Mahmode H (2012) Hydrodynamic aquifer or reservoir compartmentalization. AAPG Bull 96:315–336

Najafi M (2009) Structural evidences of Nezamabad fault effects on the Zagros fold-trust belt front. In: 11th annual meeting of Iran geological association, Theran (in Persian)

National Iranian Oil Company report (2007a) Final reservoir engineering report of Varavi gas field (unpublished report, in Persian)

National Iranian Oil Company report (2007b) Updating simulation model of Nar gasfield (unpublished report, in Persian)

National Iranian Oil Company report (2007c) Hydrodynamic study of Homa–Shanul–Varavi gas fields (unpublished report, in Persian)

National Iranian Oil Company report (2009a) Reservoir layering of Kangan gas field (unpublished report, in Persian)

National Iranian Oil Company report (2009b) Basic reservoir engineering of Kangan gasfield (unpublished report, in Persian)

National Iranian Oil Company report (2009c) Regional geology of north eastern part of Kangan Anticline (unpublished report, in Persian)

Novak K, Malvić T, Simon K (2013) Increased hydrocarbon recovery and CO_2 management, a Croatian example. Environ Earth Sci 68:1187–1197

Pelissier J, Hedayat AA, Abgrall E, Plique J (1980) Study of hydrodynamic activity in the Mishrif fields of offshore Iran. J Petrol Technol 32:1043–1052

Raeisi E (2008) Ground-water storage calculation in Karst aquifers with alluvium or no-flow boundaries. J Cave Karst Stud 70:62–70

Rahimpour-Bonab H, Esrafili-Dizaji B, Tavakoli V (2010) Dolomitization and anhydrite precipitation in Permo–Triasic carbonates at the South Pars gasfield, offshore Iran; controls on reservoir quality. J Petrol Geol 33:43–66

Saripalli KP, McGrail BP, White MD (2001) Modeling the sequestration of CO_2 in deep geological formations. First national conference on carbon sequestration, NETL, the Energy lab publication, USA

Seggie RJ, Ainsworth RB, Johnson DA, Koninx JPM, Spaargaren B, Stephenson PM (2000) Awakening of a sleeping giant: troubadour gas condensate field. APPEA J 40:417–435

Sharland PR, Archer R, Casey DM, Davies RB, Hall SH, Heward AP, Horbury AD, Simmons MD (2001) Arabian plate sequence stratigraphy. GeoArabia Special Publ 2:371

Stocklin J (1968) Structural history and tectonics of Iran: a review. AAPG Bull 52:1229–1258

Stocklin J, Setudehnia A (1977) Stratigraphic Lexicon of Iran. Geological Survey of Iran, Tehran

Szabo F, Kheradpir A (1978) Permian and Triassic stratigraphy, Zagros Basin, south-west Iran. J Petrol Geol 1:57–82

Talbot CJ (1979) Fold trains in a glacier of salt in southern Iran. J Struct Geol 1:5–18

Talbot CJ, Jarvis RJ (1984) Age, budget and dynamics of an active salt extrusion in Iran. J Struct Geol 6:521–533

Tozer RSJ, Borthwick AM (2010) Variation in fluid contacts in the Azeri field, Azerbaijan: sealing faults or hydrodynamic aquifer. Geol Soc Lond Special Publ 347:103–111

Villegas ME, Bachu S, Ramon JC, Underschultz JR (1994) Flow of formation waters in the Ceraceous-Miocene succession of the Llanos Basin, Colombia. AAPG Bull 78:1843–1862

Wells PRA (1988) Hydrodynamic trapping in the Cretaceous Nahr Umr lower sand of the north area, offshore Qatar. J Petrol Technol 40:357–367

Whitson CH, Kuntadi A (2005) Khuff gas condensate development, IPTC 10692-MS. International Petroleum Technology Conference, Doha

Yang F, Bai B, Dunn-Norman S (2011) Modeling the effects of completion techniques and formation heterogeneity on CO_2 sequestration in shallow and deep saline aquifers. Environ Earth Sci 64:841–849